Reduced timing jitter in dispersion-managed light-wave systems through parametric amplification

Jayanthi Santhanam

Department of Physics and Astronomy, University of Rochester, Rochester, New York 14627

Govind P. Agrawal

The Institute of Optics, University of Rochester, Rochester, New York 14627

We show that the timing jitter in dispersion-managed light-wave systems can be reduced considerably by replacing the erbium-doped fiber amplifiers with parametric amplifiers in which four-wave mixing is used to generate a phase-conjugated signal. We derive analytic expressions for the timing jitter by using the moment method for both the soliton and the nonsoliton systems and show that in both cases parametric amplifiers reduce the timing jitter enough that a 160-Gbit/s system is not jitter limited to distances as large as 4000 km. We include the contribution to timing jitter from the frequency shifts induced by intrapulse Raman scattering because this contribution dominates at such high bit rates. The effects of third-order dispersion are also included in the theoretical analysis. © 2003 Optical Society of America

OCIS codes: 060.0060, 060.2330, 060.2320, 060.5530, 060.4510.

1. INTRODUCTION

Light-wave transmission over long distances is limited by amplified spontaneous emission (ASE) added to optical amplifiers needed for compensation of fiber losses. The ASE induces random frequency shifts that accumulate and introduce timing jitter in the presence of group-velocity dispersion (GVD) as the signal propagates along the fiber.[1–3] The idea of using optical phase conjugation (OPC) to compensate for the effects of GVD and self-phase modulation is well known and was pursued during the 1990s.[4] It has also been shown that OPC can be used to cancel the Raman-induced frequency shift[5] induced by the phenomenon of intrapulse Raman scattering[6] and hence reduce timing jitter in light-wave systems designed by use of dispersion-decreasing fibers (DDFs).[7] The basic idea behind this jitter-compensation scheme is to replace erbium-doped fiber amplifiers (EDFAs) with parametric amplifiers, which would provide gain through four-wave mixing. Parametric amplifiers act as an optical phase conjugator, and the noise figure of such an amplifier is typically less than that of an EDFA.

At bit rates of up to 20 Gbit/s, timing jitter is due mainly to the Gordon–Haus effect.[1] But at higher bit rates the pulse width becomes so short that timing jitter is dominated by the Raman jitter caused by Raman-induced frequency shifts. It has been shown previously that, for a chain of N amplifiers, timing jitter resulting from the Raman-induced frequency shift grows as N^5 whereas the Gordon–Haus jitter grows only as N^3.[8,9] Recently we derived the analytic expressions for the timing jitter in the cases of dispersion-managed (DM) solitons, standard solitons in DDF or constant-dispersion fiber, and chirped return-to-zero (CRZ) systems.[9] In this paper we show that, by using parametric amplifiers in place of EDFAs, both the Raman and the Gordon–Haus

contributions to jitter can be reduced by a large amount in all three cases. However the effects of third-order dispersion (TOD) cannot be compensated by use of OPC.

In Section 2 we present details of parametric amplification and the OPC phenomenon. Section 3 shows how the moment method can be used to find an approximate analytic expression for timing jitter in DM light-wave systems. In Section 4 we apply this method to the case of DM solitons and consider systems designed by use of either periodic dispersion maps or DDFs. The analytic results are used to discuss the reduction in timing jitter for a 160-Gbit/s system when EDFAs are replaced with parametric amplifiers. Section 5 focuses on quasi-linear CRZ systems and shows that parametric amplifiers reduce the jitter even in this case. In Section 6 we summarize our main results and discuss their significance.

2. PARAMETRIC AMPLIFICATION

A DM system consists of a periodic sequence of anomalous- and normal-dispersion fiber sections. To compensate for fiber losses in such a system, an amplifier is placed after one or more map periods. While restoring the pulse energy to its original value, these amplifiers add spontaneous-emission noise that changes the amplitude, width, position, frequency, and phase of each pulse in a random fashion. Frequency fluctuations affect the pulse position because of GVD-induced changes in the group velocity and lead to the so-called Gordon–Haus jitter. In contrast, amplitude fluctuations lead to the Raman jitter because of intrapulse Raman scattering. It has been shown that Raman-induced jitter can dominate the Gordon–Haus effect for short pulses and hence become an important limiting factor at high bit rates.[8,9] Using parametric amplifiers in place of EDFAs one can compen-

sate for the Raman-induced frequency shift that occurs over two successive amplifier spacings.[7] Since OPC can also be used to compensate for the GVD, in this paper we show that both the Gordon–Haus jitter and the Raman-induced jitter can be reduced for DM systems by use of parametric amplifiers.

Parametric amplifiers use a four-wave mixing process[6] in which the energy of one or more pumps is used to amplify a weak signal and to generate simultaneously one or more waves at idler frequencies.[10–12] The most important feature of a parametric amplifier for our purpose is that the phase of the idler waves is related to the phase of the signal wave as $\phi_i = \phi_0 - \phi_s$ because of OPC, where ϕ_0 is a constant phase related to the pump phases. For a signal field with amplitude $A(z, t)$, the idler fields can be written as $A^*(z, t)$ within a constant phase factor. In practice, A and A^* have different wavelengths. In the case of two pumps, the three main idler frequencies are related to the signal frequency ω_s as $\omega_i = \omega_1 + \omega_2 - \omega_s$, $\omega_i' = 2\omega_1 - \omega_s$, $\omega_i'' = 2\omega_2 - \omega_s$, where ω_1 and ω_2 are the pump frequencies.[11] In practice one should choose the idler whose frequency is close to the signal frequency so that all the fiber parameters remain nearly the same for both fields. The proposed technique can tolerate a mismatch of 2 or 3 nm, especially if the dispersion slopes are matched along the DM fiber link, but is likely to become unsuitable when the signal and the idler wavelengths differ by more than 5 nm.

Consider a DM system in which parametric amplifiers are used periodically with a spacing L_A. The propagation of an optical pulse in the first fiber section before it is amplified by a parametric amplifier is governed by the following generalized nonlinear Schrödinger equation[6]:

$$i\frac{\partial A}{\partial z} - \frac{\beta_2}{2}\frac{\partial^2 A}{\partial t^2} - i\frac{\beta_3}{6}\frac{\partial^3 A}{\partial t^3} + \gamma|A|^2 A$$
$$= -\frac{i\alpha}{2}A + T_R\gamma A\frac{\partial|A|^2}{\partial t}, \quad (1)$$

where $A(z, t)$ is the slowly varying amplitude of the pulse envelope, α represents fiber losses, β_2 is the GVD coefficient, β_3 is the TOD parameter, γ is the nonlinear parameter responsible for self-phase modulation, and the Raman parameter T_R accounts for the Raman-induced frequency shift. After the signal is amplified by the first parametric amplifier, the idler field is proportional to $A^*(z, t)$ if the pump has a narrow spectrum compared with the signal. If this field is used in the next fiber section, its evolution would be governed by the following equation that we obtained by taking the complex conjugate of Eq. (1):

$$i\frac{\partial A^*}{\partial z} + \frac{\beta_2}{2}\frac{\partial^2 A^*}{\partial t^2} - i\frac{\beta_3}{6}\frac{\partial^3 A^*}{\partial t^3} - \gamma|A|^2 A^*$$
$$= -\frac{i\alpha}{2}A^* - T_R\gamma A^*\frac{\partial|A|^2}{\partial t}. \quad (2)$$

After the second amplifier, the signal goes back to $A(z, t)$ and hence would satisfy Eq. (1). It is thus evident that the evolution of each optical pulse is periodic with period $2L_A$ rather than amplifier spacing L_A.

Within each period of length $2L_A$, we need to use Eqs. (1) and (2) in the two neighboring fiber spans of length L_A. A comparison of these two equations shows that the GVD parameter β_2 and the self-phase modulation parameter γ change sign after each amplifier. Since the Raman term is proportional to γ, it also changes its sign. The net result is that the GVD, self-phase modulation, and the Raman-induced frequency shift are compensated after every two amplifiers. This is the main advantage of the use of parametric amplifiers. Since TOD does not change sign, OPC does not help to reduce the TOD effects.

3. MOMENT METHOD

Here we discuss the moment method that was used recently for the calculation of timing jitter in DM light-wave systems.[13–15] We also assume that the pulse shape can be approximated by a Gaussian function for a DM system. This is a reasonable approximation in most cases of practical interest. Numerical simulations based on Eq. (1) show that the pulse shape remains close to Gaussian except in the wings far from the center.[3] Assuming that a chirped Gaussian pulse is launched initially and maintains its Gaussian form during propagation, the optical field at any point along the fiber can be written as

$$A(z, t) = a \exp[-(1 + iC)(t - T)^2/2\tau^2$$
$$+ i\phi - i\Omega(t - T)], \quad (3)$$

where amplitude a, phase ϕ, frequency Ω, time delay T, chirp C, and width τ are all functions of z that evolve along the fiber link periodically in the case of solitons. The z dependence of these parameters can be found by use of the variational method.[16]

The three moments that represent pulse energy E, pulse position T, and frequency shift Ω can then be written as[14]

$$E = \int_{-\infty}^{\infty}|A|^2\mathrm{d}t, \quad (4)$$

$$T = \frac{1}{E}\int_{-\infty}^{\infty}t|A|^2\mathrm{d}t, \quad (5)$$

$$\Omega = \frac{i}{2E}\int_{-\infty}^{\infty}\left(A^*\frac{\partial A}{\partial t} - A\frac{\partial A^*}{\partial t}\right)\mathrm{d}t. \quad (6)$$

It is important to stress that E, T, and Ω in Eqs. (4)–(6) are not constants but evolve along the fiber link. Using Eqs. (1)–(6) we can find their evolution by solving the following set of three equations:

$$\frac{\mathrm{d}E}{\mathrm{d}z} = -\alpha E + \sum_{i=i}^{N}(g_i E + \delta E_i)\delta(z - z_i), \quad (7)$$

$$\frac{\mathrm{d}\Omega}{\mathrm{d}z} = -\frac{T_R\gamma E}{2\sqrt{\pi}\tau^3} + \sum_{i=1}^{N}\delta\Omega_i\delta(z - z_i), \quad (8)$$

$$\frac{\mathrm{d}T}{\mathrm{d}z} = \beta_2\Omega + \frac{\beta_3(1 + C^2)}{12\tau^2} + \beta_3\frac{\Omega^2}{6} + \sum_{i=1}^{N}\delta T_i\delta(z - z_i), \quad (9)$$

where the last term represents the effect of lumped amplifiers, and g_i is the gain of the ith amplifier. Random fluctuations in the pulse energy, frequency, and position added by the ith amplifier located at z_i are given by δE_i, $\delta\Omega_i$, and δT_i, respectively. The gain of each amplifier compensates fully all the fiber losses that occurred in the preceding fiber section. Since the amplifiers compensate fully all fiber losses, the energy decreases as $E_0 \exp[-\alpha(z - z_i)]$ for $z_i < z < z_{i+1}$ and recovers its input value E_0 at the next amplifier.

The variance of timing jitter is defined as $\sigma_t^2 = \langle T^2 \rangle - \langle T \rangle^2$. To find the timing jitter, we need the second moments of δE_i, $\delta\Omega_i$, and δT_i at each amplifier. These moments can be calculated by use of Eqs. (3)–(6) with $A = A + \delta A_i$, where δA_i represents the perturbation induced by the ith amplifier. This perturbation vanishes on average but its second moment is given by[3]

$$\langle \delta A_i^*(t)\, \delta A_j(t') \rangle = S\, \delta_{ij} \delta(t - t'), \qquad (10)$$

where $S = n_{sp} h\nu(G - 1)$ is the ASE spectral noise density of an amplifier with gain G,[3] n_{sp} is the spontaneous-emission factor related to the noise figure as $F_n = 2n_{sp}$, and $h\nu$ is the photon energy. The variances and cross correlations of fluctuations δE_i, $\delta\Omega_i$, and δT_i are found to be

$$\langle \delta E_i^2 \rangle = 2SE_i, \qquad \langle \delta\Omega_i \delta E_i \rangle = \frac{2SC_i}{\sqrt{\pi}\tau_i}, \qquad (11)$$

$$\langle \delta\Omega_i^2 \rangle = \frac{S(1 + C_i^2)}{E_i \tau_i^2}, \quad \langle \delta E_i \delta T_i \rangle = 0, \qquad (12)$$

$$\langle \delta T_i^2 \rangle = \frac{S\tau_i^2}{E_i}, \qquad \langle \delta\Omega_i \delta T_i \rangle = \frac{SC_i}{E_i}, \qquad (13)$$

where E_i, τ_i, and C_i are the energy, width, and chirp of the pulse at the output of the ith amplifier. In the case of DM solitons, each pulse recovers its input parameters if the amplifier spacing L_A is an integer multiple of map period L_m. In that case, the parameters E_i, C_i, and τ_i can be replaced with their initial values E_0, C_0, and τ_0, respectively.

When we use parametric amplifiers, optical field A becomes A^* after each amplifier, effectively changing the sign of C, ϕ, and Ω in Eq. (3). Hence, $\langle \delta\Omega_i \delta E_i \rangle$ and $\langle \delta\Omega_i \delta T_i \rangle$ in Eqs. (11) and (13) change sign after each amplifier. As discussed in Section 2, the pulse evolution is periodic, not after every amplifier but after every two amplifiers. We use this feature to calculate the effect of parametric amplification on the timing jitter. Consider a set of two amplifiers. Equations (7)–(9) show how E, Ω, and T evolve along the fiber link before the first amplifier. Integrating these equations over amplifier spacing L_A and including the fluctuations induced by the first amplifier, we obtain

$$E(L_A) = E(0) + \delta E_1, \qquad (14)$$

$$\Omega(L_A) = -\Omega(0) - b_R E(0) + \delta\Omega_1, \qquad (15)$$

$$T(L_A) = T(0) - b_2\Omega(0) - b_{2R}E(0) + b_3 + b_{3\Omega}\Omega^2(0)$$
$$- b_{E\Omega}E(0)\Omega(0) + b_{3E}E^2(0) + \delta T_1, \qquad (16)$$

where the sign of Ω was reversed to account for the phase reversal at the parametric amplifier. The other parameters are defined as

$$b_2 = \int_0^{L_A} \beta_2(z)\mathrm{d}z, \qquad b_3 = \int_0^{L_A} \frac{\beta_3(1 + C^2)}{12\tau^2}\mathrm{d}z, \qquad (17)$$

$$b_R = -\int_0^{L_A} q(z)\mathrm{d}z,$$

$$b_{2R} = -\int_0^{L_A} \mathrm{d}z\,\beta_2(z) \int_0^z \mathrm{d}z'\, q(z'), \qquad (18)$$

$$b_{3\Omega} = \frac{1}{6}\int_0^{L_A} \beta_3 \mathrm{d}z,$$

$$b_{E\Omega} = -\frac{1}{6}\int_0^{L_A} \mathrm{d}z\,\beta_3(z) \int_0^z q(z')\mathrm{d}z', \qquad (19)$$

$$b_{3E} = -\frac{1}{6}\int_0^{L_A} \mathrm{d}z\,\beta_3(z)\left[\int_0^z q(z')\mathrm{d}z'\right]^2,$$

$$q(z) = \frac{T_R \gamma(z) p(z)}{2\sqrt{\pi}\tau^3(z)}, \qquad (20)$$

where $p(z) = \exp[-\int_0^z \alpha(z)\mathrm{d}z]$ represents the power-reduction factor at a distance z from the last amplifier. These parameters depend on the local values of the pulse width and the chirp within the map period, which can be obtained by use of the variational analysis.[3] For simplicity in the following we neglect the higher-order terms $b_{3\Omega}$, b_{3E}, and $b_{\Omega E}$ because they involve the product of two small quantities but retain the b_3 term that depends on β_3 alone.

We now consider changes in E, Ω, and T after the first amplifier. Equations (7)–(9) can still be used if we change β_2 to $-\beta_2$ and γ to $-\gamma$ as discussed in Section 2. Integrating these equations, E, Ω, and T after the second amplifier are given by

$$E(2L_A) = E(0) + \delta E_1 + \delta E_2, \qquad (21)$$

$$\Omega(2L_A) = \Omega(0) - b_R \delta E_1 + \delta\Omega_1 + \delta\Omega_2, \qquad (22)$$

$$T(2L_A) = T(0) - b_2 b_R E(0) + 2b_3 - b_2 \delta\Omega_1$$
$$- b_{2R}\delta E_1 + \delta T_1 + \delta T_2. \qquad (23)$$

These equations show that after every two amplifiers, the effects of Raman-induced frequency shift and GVD cancel precisely because of parametric amplification. In the case of solitons, pulse parameters such as the chirp and the pulse width are also restored to their input values after every two amplifiers. Since the analysis is simpler for DM solitons, we consider this case first.

4. TIMING JITTER FOR SOLITONS

We consider a DM soliton system with N parametric amplifiers, grouped into M pairs so that $M = N/2$. We can find the average temporal shift by summing Eq. (23) over $N/2$ such pairs and performing the ensemble average. It is given by

$$\langle T(NL_A)\rangle = (N/2)[2b_3 - b_2 b_R E_0 - b_{2R}S], \quad (24)$$

where E_0 is the input pulse energy. To calculate the timing jitter, we need the variance $\langle T^2(NL_A)\rangle$ for which we need to find the variances and cross correlation of $E(NL_A)$ and $T(N_A)$ by use of Eqs. (21)–(23).

We calculated the timing jitters in the cases of both parametric and lumped amplifiers (EDFAs) and compared them to study the advantages offered by parametric amplifiers. Since the pulse energy, chirp, and pulse width are restored to their original values after every amplifier, the summation over M amplifier pairs is easily performed. The final expressions for the timing jitter in the two cases are given by

$$\sigma_{PA}^2 = \sigma_{GH}'^2 + [b_2^2 b_R^2(N^2 - 4)/12 + b_{2R}^2]N/2\langle \delta E^2\rangle$$
$$+ b_3 SN(N - 2)^2(N - 4)/96, \quad (25)$$

$$\sigma_{FA}^2 = \sigma_{GH}^2 + R_1\langle(\delta E)^2\rangle + R_2\langle\delta E\,\delta\Omega\rangle + R_3 S/E,$$
$$(26)$$

where the subscripts PA and FA stand for parametric and fiber amplifiers, respectively, and the coefficients R_1, R_2, and R_3 are given by

$$R_1 = N(N - 1)[b_R^2 b_2^2(N^3 - 10N^2 + 29N - 9)/120$$
$$+ b_2 b_R b_{2R}(19N^2 - 65N + 48)/96$$
$$+ b_{2R}^2(2N - 1)/6], \quad (27)$$

$$R_2 = N(N - 1)b_2[b_2 b_R(N - 2)(3N - 1)/12$$
$$+ b_{2R}(2N - 1)/3], \quad (28)$$

$$R_3 = N(N - 1)b_3[b_3(N - 1)(N - 2)/6$$
$$+ 4b_2(N - 1)/3\tau_0]. \quad (29)$$

The Gordon–Haus contribution to timing jitter is also different for parametric amplifiers and EDFAs and is given by

$$\sigma_{GH}'^2 = N(b_2^2/2)\langle\delta\Omega^2\rangle + N\langle\delta T^2\rangle, \quad (30)$$

$$\sigma_{GH}^2 = (b_2^2/6)N(N - 1)(2N - 1)\langle\delta\Omega^2\rangle$$
$$+ b_2 N(N - 1)\langle\delta\Omega\,\delta T\rangle + N\langle\delta T^2\rangle. \quad (31)$$

When EDFAs are used, the variance of Raman-induced timing jitter scales as N^5 and the Gordon–Haus jitter scales as N^3 with number of amplifiers.[9] It is obvious from Eqs. (25)–(31) that both the Raman jitter and the Gordon–Haus jitter are reduced considerably by use of parametric amplifiers because they scale as N^3 and N rather than N^5 and N^3, respectively.

To illustrate the extent of timing jitter reduction offered by parametric amplifiers, we consider a dense DM system capable of operating at 160 Gbit/s. The map consists of a 1-km section of anomalous GVD fiber ($D = 2.5$ ps/km nm) and another 1-km section of normal GVD fiber ($D = -2.43$ ps/km nm). In both fiber sections, $\alpha = 0.2$ dB/km, the nonlinear parameter $\gamma = 2.26$ W^{-1}/km, the Raman parameter $T_R = 3$ fs, and $\beta_3 = 0.1$ ps^3/km. Amplifiers were placed 40 km apart. The noise figure for parametric amplifiers depends on the excess noise introduced by pump power fluctuations. We calculated the spectral noise density by using $n_{sp} = 1.3$

for both parametric amplifiers and EDFAs (the worst-case situation), which corresponds to a noise figure of 4.2 dB. The parameters for the input Gaussian pulse were found by use of the periodicity conditions for solitons and have values $\tau_0 = 1.25$ ps, $C_0 = 1$, and $E_0 = 0.12$ pJ.[16] Figure 1 shows the increase in timing jitter as a function of distance in the cases of EDFAs and parametric amplifiers. The solid and dashed curves show, respectively, the total timing jitter with and without ($T_R = 0$) the Raman contribution. The dotted curve shows the tolerable value of the jitter for a 160-Gbit/s system (8% of the bit slot). In the absence of parametric amplifiers, the system performance is limited by the jitter to the extent that the soliton system cannot operate beyond 500 km. However when parametric amplifiers are used, the timing jitter is reduced so much that it limits the system performance after only 4000 km. (Of course, other effects such as soliton collisions and Q-factor degradation might not allow transmission over 4000 km.)

In another scheme for dispersion management, standard unchirped solitons are launched inside a DDF to ensure that the soliton shape and width are preserved in spite of fiber losses.[8] The GVD coefficient for DDFs decreases as $|\beta_2(z)| = |\beta_2(0)|\exp(-\alpha z)$ along the length of the fiber and reaches a value of β_2^{min} at the end of each fiber section of length L_A. Using the pulse shape in the form

$$A = a\,\text{sech}(t - T/\tau)\exp(i\phi - i\Omega t) \quad (32)$$

in Eqs. (4)–(6), we can find the variances and correlations of E, Ω, and T as before. Equations (11)–(13) are replaced with

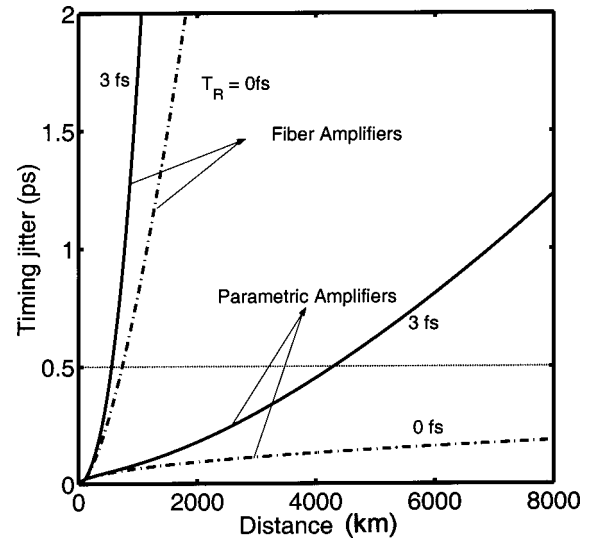$$\langle\delta E_i^2\rangle = 2SE_i, \qquad \langle\delta\Omega_i\delta E_i\rangle = 0, \quad (33)$$

Fig. 1. Timing jitter for a 160-Gbit/s DM soliton system with 40-km amplifier spacing. The solid and dashed curves show, respectively, timing jitter with and without the Raman contribution for both EDFAs and parametric amplifiers. The map parameters are given in the text and result in an average dispersion of $\beta_{av} = -0.1$ ps^2/km. The dotted curve shows the acceptable timing jitter value.

$$\langle \delta\Omega_i^2 \rangle = \frac{2S}{3E_i\tau_i^2}, \qquad \langle \delta E_i \delta T_i \rangle = 0, \qquad (34)$$

$$\langle \delta T_i^2 \rangle = \frac{\pi^2 S \tau_i^2}{6E_i}, \qquad \langle \delta\Omega_i \delta T_i \rangle = 0. \qquad (35)$$

Similarly, Eqs. (7)–(9) are replaced with

$$\frac{dE}{dz} = -\alpha E + \sum_i (g_i E + \delta E_i)\delta(z - z_i), \qquad (36)$$

$$\frac{d\Omega}{dz} = -\frac{4T_R\gamma E}{15\tau^3} + \sum_i \delta\Omega_i \delta(z - z_i), \qquad (37)$$

$$\frac{dT}{dz} = \beta_2\Omega + \frac{\beta_3}{18\tau^2} + \beta_3\frac{\Omega^2}{6} + \sum_i \delta T_i \delta(z - z_i). \qquad (38)$$

Integrating these equations, we again obtain Eqs. (21)–(23) except that the coefficients in Eqs. (17)–(20) change to

$$b_2 = \beta_2(0)L_{\text{eff}}, \qquad b_3 = \beta_3(0)L_{\text{eff}}/(18\tau^2), \qquad (39)$$

$$b_R = -4\gamma T_R L_{\text{eff}}/(15\tau_0^3), \qquad (40)$$

$$b_{2R} = -2\gamma T_R \beta_2(0)L_{\text{eff}}^2/(15\tau_0^3), \qquad (41)$$

where L_{eff} is the effective length defined as

$$L_{\text{eff}} = [1 - \exp(-\alpha L_A)]/\alpha. \qquad (42)$$

The expression for the variance of timing jitter in the case of parametric amplifiers is identical to that given in Eq. (25) earlier for DM solitons except for the different definitions of the parameters in Eqs. (39)–(41). The variance of timing jitter in the case of EDFAs is given by

$$\sigma_{\text{FA}}^2 = \sigma_{\text{GH}}^2 + R_1\langle(\delta E)^2\rangle + R_3 S/E, \qquad (43)$$

where R_1 and R_3 are defined as in Eqs. (27)–(29), and the Gordon–Haus contribution is given by

$$\sigma_{\text{GH}}^2 = (b_2^2/6)N(N-1)(2N-1)\langle\delta\Omega^2\rangle + N\langle\delta T^2\rangle. \qquad (44)$$

Comparing Eqs. (25) and (30) with Eqs. (43) and (44) we find that, similar to the case of DM solitons, parametric amplifiers reduce both the Raman jitter and the Gordon–Haus jitter. This conclusion agrees with the earlier results obtained in Ref. 7.

To determine if parametric amplification can help in the case of DDFs, we again consider the 160-Gbit/s soliton system with a 45-km-long DDF with $D(0) = 1.0$ ps/(km nm). All other parameters remain the same except for the input pulse energy, which was set to 0.9 pJ so that it corresponds to a standard fundamental soliton. Figure 2 shows the dependence of timing jitter on distance for such a system while EDFAs and parametric amplifiers are used. Similar to the DM soliton case, timing jitter limits the distance to less than 500 km when EDFAs are used. The use of parametric amplifiers reduces the jitter to within a tolerable value for distances as large as 8000 km. Again, other effects not included here could limit the distance to much smaller values.

Figures 3 and 4 show comparisons of the analytical results for DM solitons with the numerical simulations per-

formed when the nonlinear Schrödinger equation (1) was solved with the split-step method.[6] For the same map used in Fig. 1, Fig. 3 compares the Gordon–Haus timing jitter ($T_R = 0$) for EDFAs and parametric amplifiers. The solid curve shows the analytical results and the stars represent the results of numerical simulations. Figure 4 shows the total jitter including the Raman effect ($T_R = 3$ fs) under the same conditions. Numerical simulations confirm the analytical prediction that, when parametric amplifiers are used instead of EDFAs, both the Gordon–Haus jitter and the Raman-induced jitter decrease substantially. The numerical results nearly coincide with the predictions of Eqs. (25) and (26) and those of Eqs. (30) and (31). The small discrepancies seen in Figs.
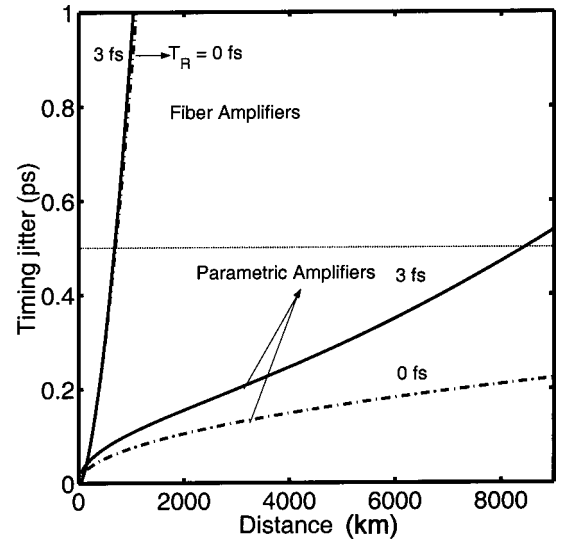

Fig. 2. Same as Fig. 1 except that the system was designed by use of DDFs and amplifiers are placed every 45 km. The GVD decreases exponentially over 45 km starting from its initial value of 1 ps/(km nm).
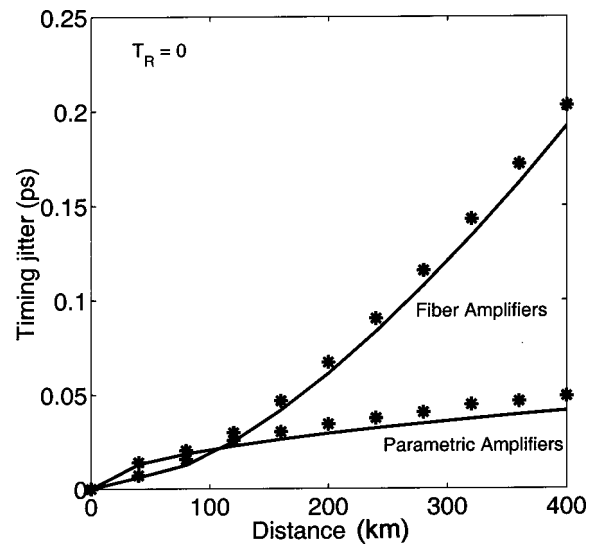

Fig. 3. Comparison of numerical (stars) and analytic (solid curve) results for $T_R = 0$ (no Raman jitter) for a 160-Gbit/s DM soliton system designed with 40-km amplifier spacing and $\beta_{\text{av}} = -0.1$ ps²/km. The dispersion map is the same as in Fig. 1.
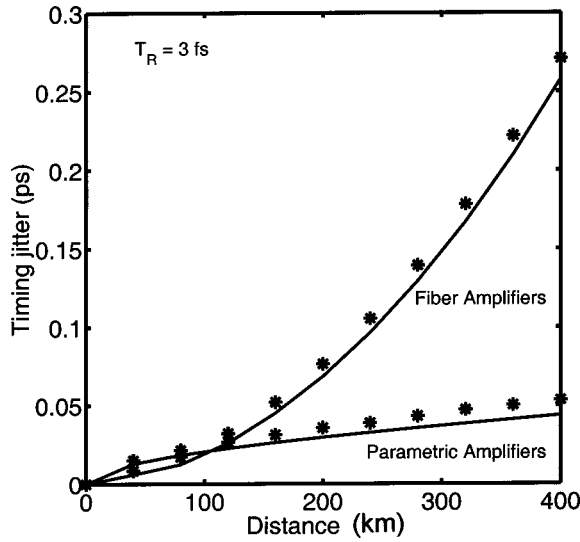
Fig. 4. Same as Fig. 3 except the Raman contribution to timing jitter is included by use of $T_R = 3$ fs. The stars and solid curves show the numerical and analytic results, respectively.

3 and 4 are due to intrapulse interaction that is not considered in the analysis but is automatically included in numerical simulations.

5. TIMING JITTER FOR CHIRPED RETURN-TO-ZERO SYSTEMS

We now focus on CRZ systems in which prechirped pulses of relatively low energy are propagated along a DM link without enforcing a periodic evolution pattern. The chirp and the pulse width cannot be calculated at the location of each amplifier in the general case in which the nonlinear effects are included. However, in the case of quasi-linear propagation, the nonlinear term in Eqs. (1) and (2) can be neglected, and the pulse evolution is nearly linear along the DM link. The chirp and the pulse width of the pulses can then be found analytically.[1] Since the noise variances and cross correlations in Eqs. (11)–(13) depend on chirp and pulse width at each amplifier, they differ for different amplifiers. After the first parametric amplifier, the chirp changes sign and is given by

$$C_1 = -(C_0 + b_2/\tau_{\min}^2), \qquad (45)$$

where $\tau_{\min}$ is the minimum pulse width in the first fiber span (equal to the width of the pulse at the transmitter before it is chirped) and is related to the input pulse width after chirping as $\tau_0^2 = \tau_{\min}^2(1 + C_0^2)$. After the second amplifier, chirp C is restored to C_0. Physically, the effect of dispersion is canceled for each pair of parametric amplifiers. Similarly, the pulse width after the first and second parametric amplifiers is given by

$$\tau_1 = \tau_{\min}\sqrt{1 + C_1^2}, \quad \tau_2 = \tau_0. \qquad (46)$$

We note from Eqs. (45) and (46) that both the chirp and the pulse width are restored to their original values after every two amplifiers just like in the case of solitons. This feature is quite different compared with the case of ED-FAs for which the width and the chirp evolve in a nonpe-

riodic fashion, because, even when the average dispersion is not zero, its effects are canceled for every pair of parametric amplifiers.

Using Eqs. (45) and (46) in Eqs. (11)–(13) with Eqs. (21)–(23) and following the procedure outlined above, we can find the variance of timing jitter in the cases of both parametric amplifiers and EDFAs in terms of the total number of amplifier N. The results are given by

$$\sigma_{\text{PA}}'^2 = \sigma_{\text{GH}}'^2 + N/2[b_2^2 b_R^2 N(N^2 - 4)/12 + b_{2R}^2 N]\langle \delta E^2 \rangle$$
$$+ b_3 SN(N - 2)(N - 4)/96E, \qquad (47)$$

$$\sigma_{\text{FA}}^2 = \sigma_{\text{GH}}^2 + R_1\langle(\delta E)^2\rangle + \frac{2S}{\sqrt{\pi}\tau_{\min}}(1 + C_0^2)^{-1/2}[R_2'C_0$$
$$- R_2'b_2(1 + 2C_0^2)/\tau_{\min}^2] + R_3'S/E. \qquad (48)$$

The Gordon–Haus contributions in the two cases are given by

$$\sigma_{\text{GH}}'^2 = N(S/E)\tau_{\min}^2[1 + b_2^2/\tau_{\min}^4 + C_0^2 + C_0 b_2/\tau_{\min}^2], \qquad (49)$$

$$\sigma_{\text{GH}}^2 = N(S/E)\tau_{\min}^2[1 + (C_0 + b_2 N/\tau_{\min}^2)^2], \qquad (50)$$

and the quantities R_2', R_2', and R_3' are defined as

$$R_2' = N(N - 1)b_2[b_2 b_R(N - 1)^2/3 + b_{2R}(2N - 1)/3], \qquad (51)$$

$$R_2' = N(N - 1)b_2[b_2 b_R(12N^3 - 40N^2 - 53)/10$$
$$+ b_{2R}(9N^2 - 3N - 13)]/18, \qquad (52)$$

$$R_3' = N(N - 1)b_3\{b_3(N - 1)(N - 2)/6$$
$$+ (4b_2/3\tau_{\min})(1 + C_0^2)^{-1/2}$$
$$\times [C_0/2 - (2N - 1)(1 + 2C_0^2)(b_2/3\tau_{\min}^2)]\}. \qquad (53)$$

In the case of EDFAs, precompensation or postcompensation of GVD can be used to reduce the variance of timing jitter to linear dependence in N.[13] For parametric amplification, the Gordon–Haus jitter is minimum when $C_0 = -b_2/2\tau_{\min}^2$. After precompensation, the resulting expressions for timing jitter become

$$\sigma_{\text{GH}}'^2 = N(S/E)\tau_{\min}^2[1 + 3b_2/4\tau_{\min}^2], \qquad (54)$$

$$\sigma_{\text{GH}}^2 = N(S/E)\tau_{\min}^2. \qquad (55)$$

Similar to the case of DM solitons, the timing jitter can be reduced by use of parametric amplifiers in place of ED-FAs. Figure 5 shows the effect of intrapulse Raman scattering on the performance of a 160-Gbit/s CRZ system by use of the same dispersion map that was used for Fig. 1. The pulse energy is reduced by a factor of 10 to reduce the nonlinear effects. We also reduced the average dispersion to $\beta_{\text{av}} = -0.005$ ps^2/km by changing the normal GVD to -2.492 ps/(km nm). In the case of EDFAs, the input chirp C_0 was chosen to be $|\beta_{\text{av}}|L/\tau_{\min}^2$, where L is the total distance of propagation.[13] For systems with parametric amplifiers C_0 was chosen to be $|\beta_{\text{av}}|L/2\tau_{\min}^2$. As expected, for light-wave systems designed by use of EDFAs, precompensation reduces the Gordon–Haus contribution but the Raman jitter increases with distance
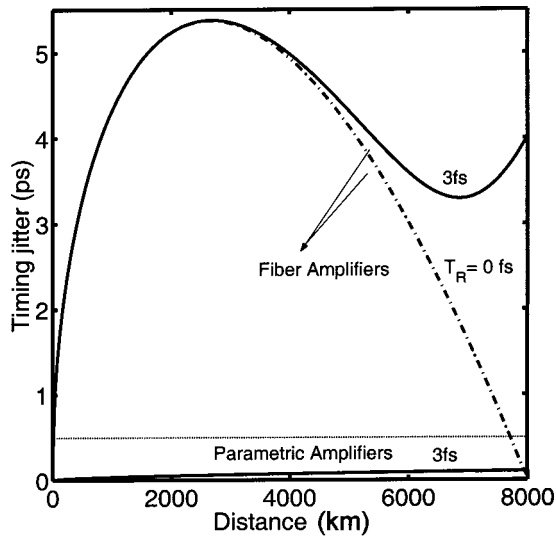
Fig. 5.   Timing jitter for a quasi-linear CRZ system with 40-km amplifier spacing and $\beta_{av} = -0.005$ ps^2/km.   The solid and dashed curves show, respectively, timing jitter with and without the Raman contribution for both EDFAs and parametric amplifiers.   The dotted line shows the acceptable timing jitter value.

and ultimately limits the system after 3000 km.   The use of parametric amplifiers reduces the Raman jitter considerably, and the system is not limited by jitter for distances as large as 10,000 km.   We again stress that other degradation factors not included here might limit the length to much smaller values even when parametric amplifiers are used.

6. SUMMARY

We have used the moment method to show that both the Raman-induced and the ASE-induced timing jitter can be reduced considerably for DM light-wave systems by replacing EDFAs with parametric amplifiers.   We were able to obtain analytic expressions for the timing jitter assuming that each optical pulse maintained a Gaussian shape even though its amplitude, width, and chirp varied along the DM fiber link.   Our expressions can be used even in the case of dense dispersion management, realized by use of multiple map periods between two neighboring amplifiers.   We have included the effects of third-order dispersion as well in this paper.

We have applied the general formalism to three types of light-wave system corresponding to the use of DM solitons, standard solitons with DDFs, and CRZ pulses in a quasi-linear configuration.   We were able to obtain the analytic expressions for the timing jitter in each case. We compared the three configurations for a 160-Gbit/s system and found that in all cases the timing jitter at the receiver end can be reduced by a large factor by replacing EDFAs with parametric amplifiers.   Although parametric amplifiers have not yet been used to design light-wave systems, the situation is likely to change in the near future in view of the recent advances in the design of broadband parametric amplifiers.[10–12]

Several assumptions made in our analysis must be satisfied before the jitter-reduction scheme of this paper can be implemented successfully.   First, the OPC process

must create a phase-conjugated version of the signal, which is possible only if the pump phase does not fluctuate significantly.   In practice, the linewidth of semiconductor lasers used for pumping is increased to ~1 GHz for suppression of the onset of stimulated Brillouin scattering.   This is not of much concern for the following reason. At high bit rates considered in this paper, each optical pulse is so short (~1 ps) that the pump phase remains constant over its entire width.   Thus, as long as the bit rate is much larger than the pump bandwidth, the OPC process is close to being ideal.   The second issue is related to the mismatch between the signal and the idler wavelengths.   The main requirement here is that the dispersion parameter should be the same at both fields, which is possible only if they have the same wavelength. In practice, the wavelength can differ by a few nanometers especially for fibers with low dispersion slopes, but larger differences are likely to become intolerable.

REFERENCES

1. G. P. Agrawal, *Fiber-Optic Communication Systems*, 3rd ed. (Wiley, New York, 2002).
2. E. Iannone, F. Matera, A. Mecozzi, and M. Settembre, *Nonlinear Optical Communication Networks* (Wiley, New York, 1998), Chap. 5.
3. G. P. Agrawal, *Applications of Nonlinear Fiber Optics* (Academic, San Diego, Calif., 2001).
4. S. Watanabe and M. Shirasaki, "Exact compensation for both chromatic dispersion and Kerr effect in a transmission fiber using optical phase conjugation," J. Lightwave Technol. **14**, 243–248 (1996).
5. S. Chi and S. Wen, "Recovery of the soliton self-frequency shift by optical phase conjugation," Opt. Lett. **19**, 1705–1707 (1994).
6. G. P. Agrawal, *Nonlinear Fiber Optics*, 3rd ed. (Academic, San Diego, Calif., 2001).
7. R. J. Essiambre and G. P. Agrawal, "Timing jitter of ultrashort solitons in high-speed communication systems. II.   Control of jitter by periodic optical phase conjugation," J. Opt. Soc. Am. B **14**, 323–330 (1997).
8. R. J. Essiambre and G. P. Agrawal, "Timing jitter of ultrashort solitons in high-speed communication systems.   I. General   formulation   and   application   to   dispersion-decreasing fibers," J. Opt. Soc. Am. B **14**, 314–322 (1997).
9. J. Santhanam and G. P. Agrawal, "Raman-induced timing jitter   in   dispersion-managed   communication   systems," IEEE J. Sel. Top. Quantum Electron. **8**, 632–639 (2002).
10. M. E. Marhic, F. S. Yang, M. C. Ho, and L. G. Kazovsky, "High-nonlinearity fiber parametric amplifiers with periodic dispersion compensation," J. Lightwave Technol. **17**, 210–215 (1999).
11. C. J. McKinstrie, S. Radic, and A. Chraplyvy, "Parametric amplifiers driven by two pump waves," IEEE J. Sel. Top. Quantum Electron. **8**, 538–547 (2002).
12. J. Hansryd, P. A. Andrekson, M. Westlund, J. Li, and P. O. Hedekvist, "Fiber-based optical parametric amplifiers and their applications," IEEE J. Sel. Top. Quantum Electron. **8**, 506–520 (2002).
13. J. Santhanam, C. J. McKinstrie, T. I. Lakoba, and G. P.

Agrawal, "Effects of precompensation and postcompensation on timing jitter in dispersion-managed systems," Opt. Lett. **26**, 1131–1133 (2001).

14. V. S. Grigoryan, C. R. Menyuk, and R. M. Mu, "Calculation of timing and amplitude jitter in dispersion-managed optical fiber communications using linearization," J. Lightwave Technol. **17**, 1347–1356 (1999).

15. C. J. McKinstrie, J. Santhanam, and G. P. Agrawal, "Gordon–Haus timing jitter in dispersion-managed systems with lumped amplification: an analytical approach," J. Opt. Soc. Am. B **19**, 640–649 (2002).

16. S. K. Turitsyn, I. Gabitov, E. W. Laedke, V. K. Mezentsev, S. L. Musher, E. G. Shapiro, T. Schafer, and K. H. Spatschek, "Variational approach to optical pulse propagation in dispersion compensated transmission systems," Opt. Commun. **151**, 117–135 (1998).